SURFACE DISCHARGES ON TEFLON, MYLAR AND KAPTON

K.G. Balmain and G.R. Dubois
Department of Electrical Engineering
University of Toronto
Toronto, Canada M5S 1A4

Abstract

FEP Teflon, Mylar and Kapton H are compared from
the point of view of charged-area scaling of discharge
current pulse properties. The properties measured are
peak current, pulse duration, released charge and en-
ergy dissipated in a load resistor, all for 20 keV in-
cident electrons at a current density of 80 nA/cm^2. In
general it is found that the three materials are more
similar than dissimilar, and furthermore that this sim-
ilarity extends to discharge damage as well, the damage
being identified as a combination of subsurface filam-
entary tunnels and surface grooves. The experimental
observations are used to motivate a theory of discharge
arc propagation in which the propagation velocity is
controlled by the rate of removal of excess charge via
wave propagation along a filamentary tunnel filled with
an overdense plasma.

Introduction

Spacecraft charging by energetic electrons and con-
sequent arc discharging of dielectric materials are now
well-established phenomena, for which a great deal of
evidence exists[1,2,3,4]. Laboratory simulation of these
phenomena has revealed that the discharges are very
strong in terms of the replacement current pulse indu-
ced in the conductors supporting the dielectric mater-
ials. The peak current and as well the released charge,
released energy and pulse duration have been found to
follow well defined scaling laws as the specimen area
is varied[5,6,7]. In addition, discharge surface damage
in the form of grooves and subsurface damage due to
discharge "tunneling" have been identified on Mylar[6]
and on Teflon[7], damage which can be widely distributed
with a web-like appearance[8].

The present study is concerned with discharge area
scaling and discharge surface and subsurface damage due
to a 20 keV beam of electrons incident on FEP Teflon,
Mylar and Kapton H. One purpose of the study is to com-
pare these three polymeric materials which are in com-
mon use on spacecraft, identifying differences or simi-
larities in their discharge behaviour. Another purpose
is to use the experimental results to suggest a theor-
etical model for the phenomenon of discharge propaga-
tion.

The Experiment

The apparatus is the same as used in previous
work[6], and is shown in Fig. 1. The charged area on the
dielectric sheet specimen is defined by a tight-fitting
circular-aperture aluminium mask which has a bevelled
edge to reduce emitted-electron interception. The mask
and the copper backing plate are connected electrically
together and both are connected to a 10-ohm load resis-
tor consisting of four 50-ohm shunts and the 50-ohm
measurement line. The discharge current as a function
of time was deduced from photographs of the current
trace on a 400 MHz bandwidth oscilloscope. A constant
beam accelerating voltage of 20 kV was used, and also a
constant incident electron beam current density of
80 nA/cm^2. The beam current density variation over the
specimen was approximately ±15% for the largest mask
aperture.

The essential experimental features of charging

and discharging are suggested in Fig. 2. The incident
electrons become embedded in the dielectric in a layer
5 to 8 μm below the surface, with resultant high elec-
tric fields being set up both above and below the charge
layer[9,10] and adjacent to the mask edge. At any of
these points breakdown may occur, resulting in a punch-
through arc to the substrate (bulk breakdown), a blow-
off arc to the surface, or a flashover arc consisting
of a propagation subsurface discharge terminating in
either a blowoff arc or punchthrough arc.

The experiment as depicted in Fig. 2 involves a
measurement of the voltage across the load resistor R,
and the current through R is contributed to significan-
tly only by blowoff of those charged particles (prim-
arily electrons) which actually reach the vacuum cham-
ber wall. The fraction of the total current intercep-
ted by the mask was not measured in these experiments.

The dielectric sheet test specimens were changed
at every change in mask aperture area in order to min-
imize the effects of accumulated damage. The materials
used were transparent FEP Teflon 50 μm thick, Mylar
75 μm thick (not from the same stock as in previously
reported work[6]), and Kapton H 75 μm thick. The dielec-
tric sheets were not metallized.

Area Scaling of Discharge Current

The properties of the discharge current pulse have
been shown[5,6,7] to have a power-law dependence on diel-
ectric specimen area, a dependence which permits easy
extrapolation from small-scale laboratory experiments
to large-scale spacecraft-size areas of dielectric. The
peak discharge current for Mylar, for example, in pre-
vious work[6] was found to scale with area in proportion
to the area raised to the power 0.50, or in other words
0.50 was the slope of the corresponding log-log graph.

For this comparison study the peak currents are
shown in Fig. 3, in which the vertical bars indicate the
ranges of values measured. The Mylar slope of 0.59 is
somewhat higher than measured previously, while the
Kapton peak currents are slightly lower and exhibit
more scatter in comparison with the other two materials.
The discharge-current pulse-duration graphs are shown in
Fig. 4, all of them being similar, with the Mylar graph
having a slope of 0.46 in comparison with the previou-
sly measured value of 0.55. If one assumes that the
pulse duration is the time required for the discharge
arc to propagate a distance equal to the mask aperture
radius, then Fig. 4 gives arc velocities of the order
of 3×10^5 m/s as measured previously[6]. The released
charge graphs of Fig. 5 exhibit relatively little scat-
ter and are similar to each other, with the Mylar graph
having a slope of 1.05 in comparison with the previous
value of 1.00. As for the energy dissipated in the
load resistor, the graphs of Fig. 6 show the Kapton en-
ergies to be slightly lower than for the other two
materials, while the Mylar graph has a slope of 1.62 in
comparison with the value of 1.49 previously measured.

Discharge Damage

Discharge damage was imaged using three techniques,
scanning-electron microscopy, transmitted-light micro-
scopy and reflected-light microscopy. Figure 7 for
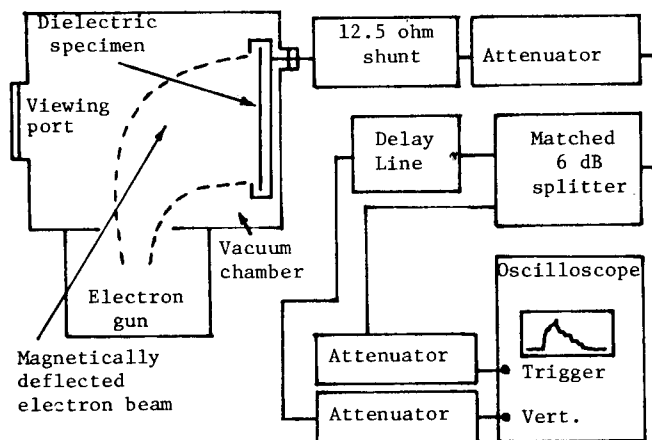Teflon shows a network of damage tunnels, some of them
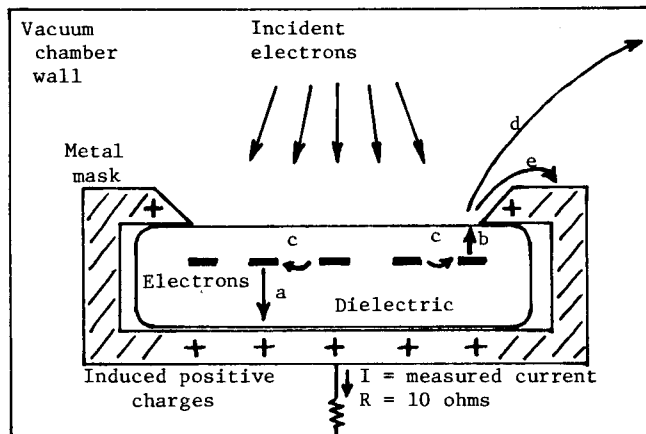
FIG. 1 Experimental apparatus

FIG. 2 Possible charging and discharging phenomena: a) punchthrough arc with top surface of dielectric blown off, b) blowoff arc to surface, c) flashover arc or propagating subsurface discharge, d) ejected electrons going to chamber wall, e) ejected electrons going to mask.
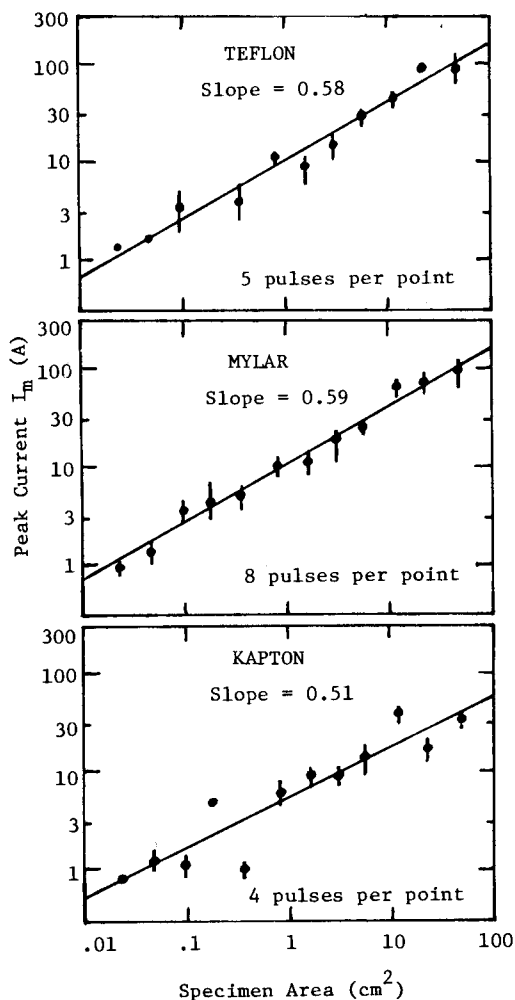

FIG. 3 The variation of peak current I_m with dielectric specimen area.
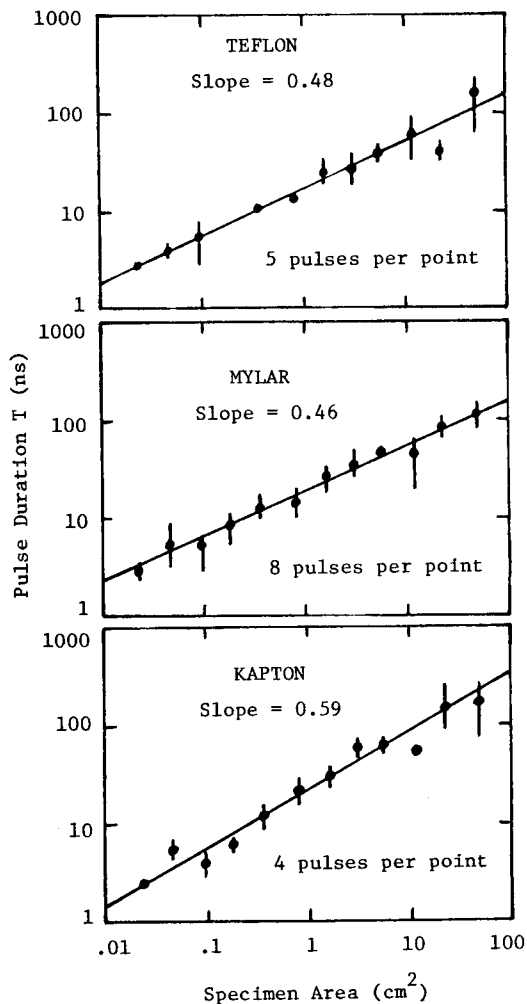

FIG. 4 The variation of pulse duration $T = \dfrac{1}{I_m} \int I \, dt$ with specimen area
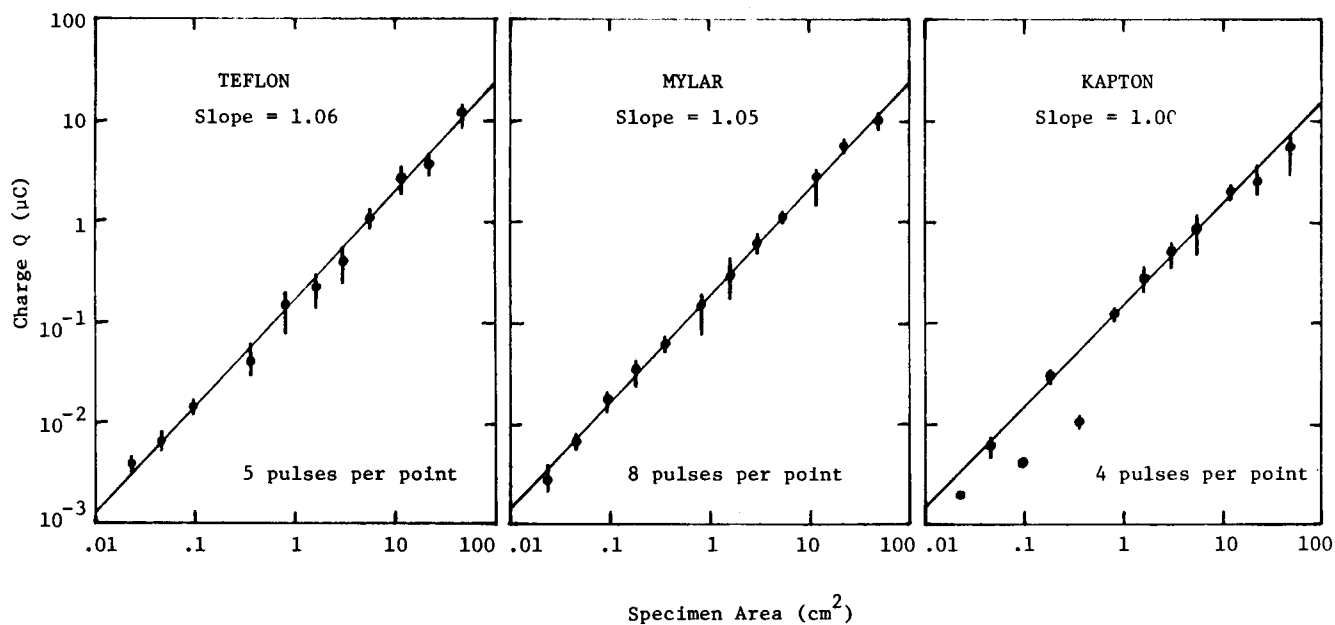
5147

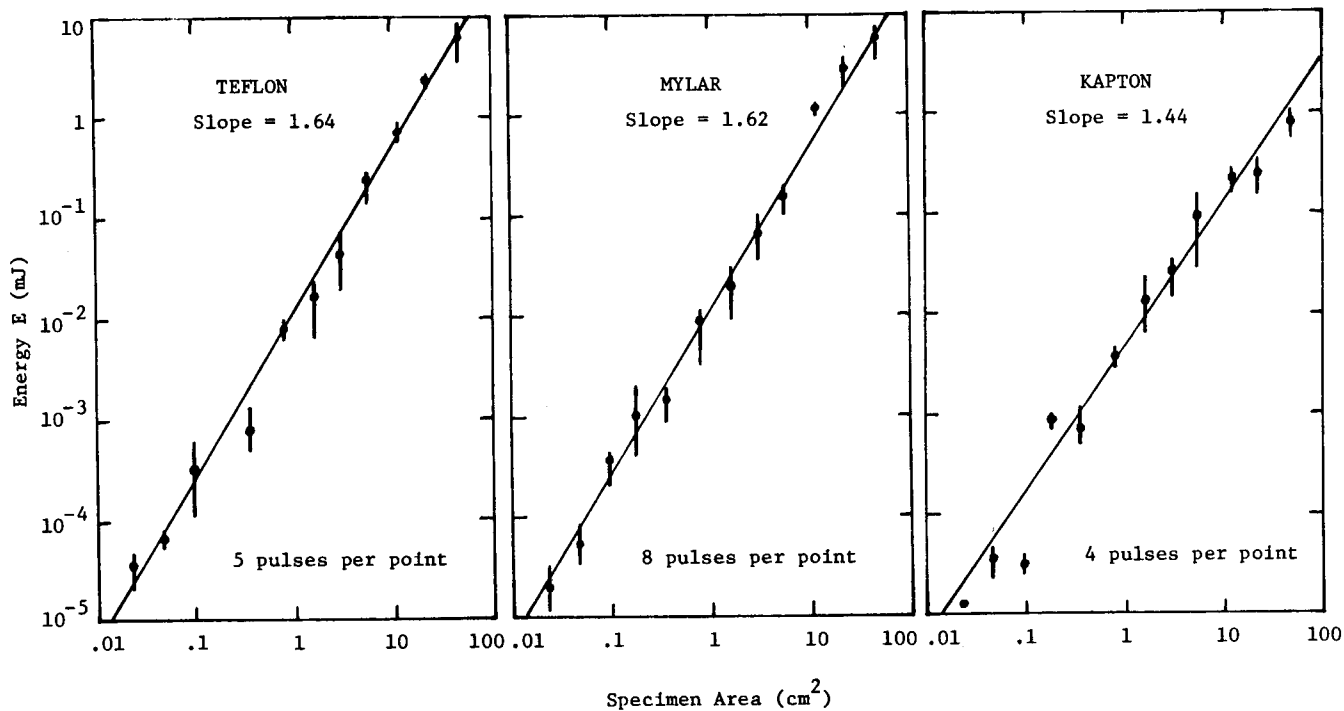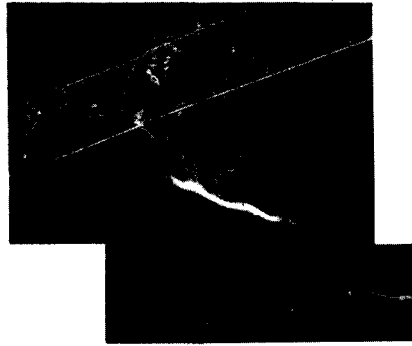FIG. 5 The variation of released charge $Q = \int I\,dt$ with dielectric specimen area.

FIG. 6 The variation of energy $E = R\int I^2 dt$ with dielectric specimen area. The energy is dissipated in a load resistor $R = 10$ ohms.
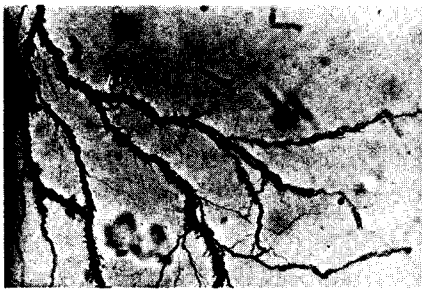
S.E.M.; 10 μm = ⊢⊣
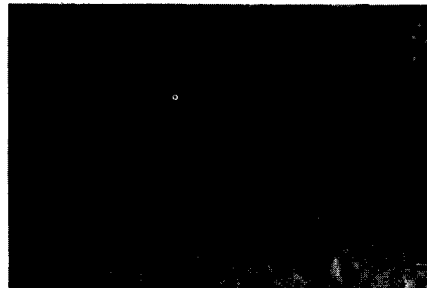
S.E.M.; 10 μm = ⊢⊣

S.E.M.; 10 μm = ⊢━━━⊣

Transmitted light; 10 μm = ⊢⊣

Transmitted light; 10 μm = ⊢⊣

Transmitted light; 10 μm = ⊢⊣
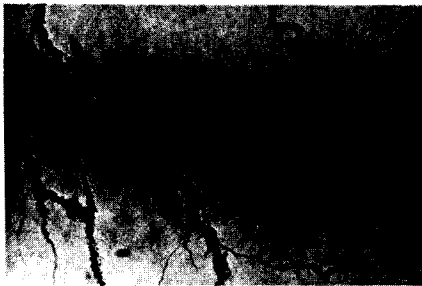
Reflected light; 10 μm = ⊢⊣

Reflected light; 10 μm = ⊢⊣

Reflected light; 10 μm = ⊢⊣

FIG. 7 Teflon discharge damage after 9 discharges with a beam density of 80 nA/cm^2. Thickness=50 μm.

FIG. 8 Mylar discharge damage after 12 discharges with a beam density of 80 nA/cm^2. Thickness = 75 μm.

FIG. 9 Kapton discharge damage after 11 discharges with a beam density of 80 nA/cm^2. Thickness=75 μm.
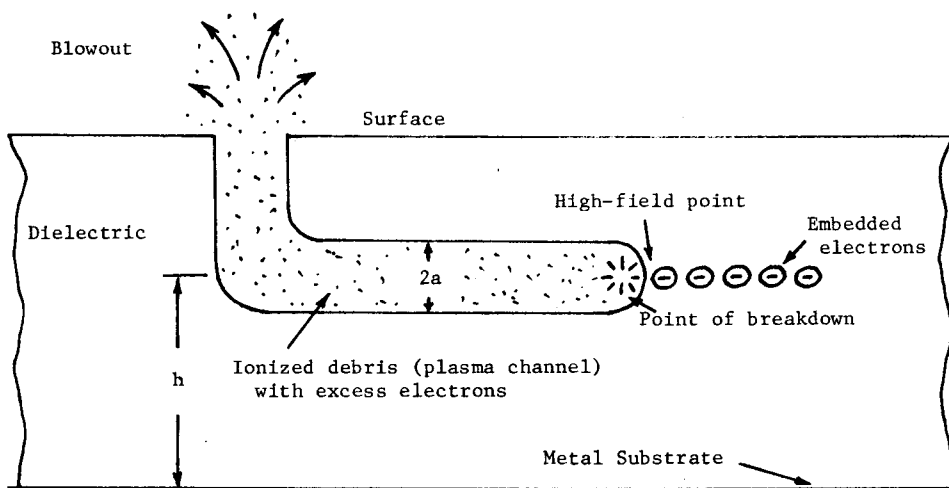
FIG. 10 The overdense plasma channel concept of discharge propagation.

completely subsurface and some over which the surface is heaved, cracked or blown out. In Fig. 7 the mask edge coincided with the upper border of the SEM photograph. There were very few such patterns, those which could be found being either near the mask edge or beside a punchthrough. Also faintly visible on the Teflon (not shown) were some straight-line surface grooves apparently caused by the discharges.

Figure 8 for Mylar shows a great variety of surface damage. Included are subsurface tunnels, heaved-surface tunnels, and blowout holes. Also clearly in evidence are surface grooves which are of two types: straight, deep, branching grooves (they are not pre-existing scratches), and very fine, irregular, tree-like grooves. The Mylar damage was extensive and easy to find, especially near the mask edge.

Figure 9 for Kapton exhibits surface grooves which are mostly straight, along with irregular subsurface tunnels, some with extensive heaving of the dielectric surface. In general, the damage was fairly widespread near the mask edge. In the case of Kapton it was particularly noticeable that surface grooves often merged with tunnels, suggesting that the two types' of damage arise from the same basic phenomenon.

One observation is common to all three materials, namely that the straight, branching damage tracks are all grooves on the surface, while the subsurface tunnels are always somewhat irregular in shape. This suggests that crystallization, which is common in polymers[11], may occur at the dielectric surface and may influence discharge propagation.

A Theory of Discharge Propagation

The foregoing experimental results on discharge pulse properties and surface damage indicate that the three dielectrics examined do not differ greatly. This suggests that a first-order theory of discharge propagation may not need to include information on the detailed molecular structure of particular polymers. The frequent observation of a network of damage tunnels and the bright, spider-web appearance of typical discharge arcs suggests that plasma-filled tunnels may cover a significant portion of the discharged surface, even though some of these tunnels may not leave behind easily visible permanent damage. It is worth noting that the formation of gaseous, ionized, conducting channels has been postulated by Budenstein[12] as an essential part of solid dielectric breakdown, and furthermore, plasma emission from discharge arcs has already been measured[7].

The inductance and capacitance of a highly conducting subsurface arc have been calculated by Leadon and Wilkenfeld[13] and by Leadon (personal communication) in order to estimate the time duration of a discharge. If the propagation of an electromagnetic wave along a subsurface arc were to determine the propagation velocity of the arc, then the inductance and capacitance of a highly conducting arc would predict propagation at the velocity of light in the dielectric. However the arc propagation velocity is estimated to be 3×10^5 m/s. Therefore it appears that some form of wave slowing would be required in the theoretical model, perhaps provided by the additional inductance per unit length of an arc which is not a perfect conductor but rather an overdense plasma.

Suppose that a breakdown occurs at a subsurface point in a dielectric, due to the presence of a high concentration of embedded charge. Further, suppose that the resulting arc propagates in one direction while the debris is ejected in the opposite direction along a filamentary tunnel. Now suppose that the discharge debris is ionized by the energy released in the discharge process. Thus the point at which the discharge occurs is linked to the outside world by a plasma channel, as indicated in Fig. 10.

Imagine the breakdown process to be a sequence of

single breakdowns. After one such breakdown the excess charge must be removed via the plasma channel before the field ahead of the point of breakdown can rise to a level high enough to produce the next breakdown. Therefore it is the rate of removal of charge which determines the rate at which the breakdown process is permitted to proceed. In the time interval between breakdowns, the distance travelled by the propagating excess charge should be about equal to the length of the high-field region built up in the solid, so the velocity of progression of the arc should be about equal to the velocity of propagation of the charge. The breakdown process is by definition highly non-linear and complex, but the propagation of excess charge dhown the plasma channel conceivably could be much closer to linearity.

Suppose then that the rate of increase of field at the high-field point is controlled by the propagation away from it of charge in the form of an electromagnetic wave along a plasma channel over a metal substrate. Such a configuration has the appearance of a transmission line, customarily regarded as having an inductance per metre given by L and a capacitance per metre given by C, where for a perfectly-conducting channel,

$$C = 2\pi\epsilon/[\cosh^{-1}(h/a)] \text{ and } L = (\mu/2\pi)\cosh^{-1}(h/a)$$

and the wave propagation velocity is $v = (LC)^{-\frac{1}{2}} = (\mu\epsilon)^{-\frac{1}{2}}$ which is the velocity of light in the dielectric medium.

Now consider a plasma channel with a relative permittivity given by $\epsilon_r = 1 - \omega_p^2/\omega^2 \approx -\omega_p^2/\omega^2$ in the overdense case, where ω is the wave frequency (radians/s) for an $\exp(j\omega t)$ time variation, $\omega_p = (Ne^2/m\epsilon_0)^{\frac{1}{2}}$ is the plasma frequency, N is the electron density (m^{-3}), e is the electron charge magnitude (coul.), m is the electron mass (kg), and ϵ_0 is the permittivity of a vacuum. Let us regard the above relative permittivity as describing completely the microscopic electrodynamics in a cylindrical conducting channel of diameter 2a. A rigorous formulation for the inductance per unit length of a cylindrical wire is well known[14], and substitution into this formulation of the above permittivity yields the inductance per unit length L_p of the plasma channel:

$$L_p = (\pi a^2 \epsilon_0 \omega_p^2)^{-1} = m(\pi a^2 Ne^2)^{-1}$$

For the parameters of interest, it may be shown readily that the field penetration depth is much greater than the channel radius, and that the other contributions to the internal and external inductance are negligible. Thus the plasma inductance per unit length L_p is independent of frequency, so that there is no pulse dispersion and an electromagnetic wave will propagate undistorted at the plasma channel velocity $v_p = (L_p C)^{-\frac{1}{2}}$, on the assumption that the capacitance per unit length is the same as in the case of a good conductor.

Not knowing N, we cannot calculate v_p. Rather than estimating N and deducing an estimated v_p, let us take an experimental value for v_p and use it to deduce N or the more convenient plasma frequency ω_p (f_p in Hz). The above expressions for plasma channel inductance and velocity give

$$\omega_p^2 = C v_p^2/\pi a^2 \epsilon_0 = 2 \epsilon_d v_p^2/a^2 \cosh^{-1}(h/a)$$

where ϵ_d is the relative permittivity of the dielectric. Setting $\omega_p = 2\pi f_p$ and approximating for large h/a, we get $f_p \approx v_p \sqrt{\epsilon_d} /2\pi a \sqrt{\ln(2h/a)}$. Taking

$$\epsilon_d \sim 3$$

$$h \sim 6 \times 10^{-5} \text{ m (typical of material thickness)}$$

$$a \sim 3 \times 10^{-7} \text{ m (from photographs of tunnels)}$$

we find $\sqrt{\epsilon_d}/\sqrt{\ln(2h/a)} \approx 1/\sqrt{2}$ and is slowly varying. Then, taking $v_p = 3 \times 10^5$ m/s, we get $f_p \sim 10^2$ GHz.

Consider now some reasonable lower and upper limits for f_p. The fastest rise and fall times yet measured for discharge pulses are 0.2 ns[15] or at the limit of a 4 GHz oscilloscope. Thus the plasma frequency f_p would have to be at least about 10 GHz. For upper limits, one might consider a poor conductor with $N \sim 10^{28}/m^3$ ($f_p \sim 10^6$ GHz), a semiconductor with $N \sim 10^{20}/m^3$ ($f_p \sim 10^2$ GHz), or a 4%-ionized gas at N.T.P. ($f_p \sim 10^4$ GHz). Therefore it would appear that the value $f_p \sim 10^2$ GHz is not unreasonable.

Conclusions

It has been shown that surface discharges on Kapton and Teflon exhibit the same type of power-law area scaling of current pulse properties as in the case of Mylar. The graphs of peak current, pulse duration, released charge and energy dissipated in a load resistor are similar for all three materials, although the peak current and energy are slightly lower in the case of Kapton. The points on the area-scaling graphs exhibit some scatter, indicating the importance in any such experiment of including at least three or four different areas for a given type of material. The possible dependence of the area scaling graphs on incident current density remains an open question following the recent observation[16] of dependence of released charge on current densities below 8nA/cm^2 (which are representative of the magnetosphere). Our own experiments suggest no noticeable dependence (except for discharge frequency) from 75 nA/cm^2 to 10 μA/cm^2.

Comparing damage in the three types of material, one notes a general similarity, with differences in detail. The most surprising detail is that the surface groove damage is mostly in the form of straight branching lines while the subsurface tunneling is irregular, suggesting that the top micron or so of the material may be significantly different from the deeper material. Surface crystallization is suggested as a possible explanation.

The combined results for discharge peak current and damage suggest that the three materials exhibit more similarity than dissimilarity, a result which could be significant both for the practical problem of materials selection and for the theoretical problem of creating mathematical models for charging and discharging phenomena.

One such theoretical model is proposed, namely the discharge arc propagation model involving the formation of filamentary plasma-filled tunnels. In this model the progress of the nonlinear arc breakdown through the material is controlled by the linear phenomenon of excess charge removal from the breakdown site via an electromagnetic wave propagating undistorted along an overdense plasma filament. Order-of-magnitude calculations tend to support this hypothesis. The plasma channel theory emphasizes subsurface effects, in contrast to the electron-hopping, secondary-emission-controlled discharge model proposed by Inouye and Sellen[17]. If the plasma channel theory were to be generally applicable then it would be necessary to postulate that many of the discharge filaments do not leave visible permanent damage, or alternatively to invoke other discharge propagation mechanisms for the sometimes very extensive dielectric areas which show no sign of the tunnel or groove forms of permanent discharge damage.

References

1. Rosen, A. (Ed.), Spacecraft Charging by Magnetospheric Plasmas, Progress in Astronautics and Aeronautics, Vol. 47, 1976.
2. Pike, C.P., and Lovell, R.R. (Eds.), Proceedings of the 1976 Spacecraft Charging Technology Conference, Report AFGL-TR-77-0051/NASA TMX-73537, 24 Feb. 1977.
3. Goodman, J.M. (Ed.), Effect of the Ionosphere on Space and Terrestrial Systems, Proceedings of an NRL/ONR-sponsored conference held in Arlington, Va., January 24-26, 1978. U.S. Gov't. Printing Office Stock No. 008-051-00069-1.
4. Spacecraft Charging Technology - 1978, Proceedings of a conference held at Colorado Springs, Oct. 31 to Nov. 2, 1978, edited by R.C. Finke and C.P. Pike, NASA Conference Publication 2071/AFGL-TR-79-0082.
5. Balmain, K.G., Kremer, P.C., and Cuchanski, M., "Charged-Area Effects on Spacecraft Dielectric Arc Discharges", in Reference 3, pp. 302-308.
6. Balmain, K.G., "Scaling Laws and Edge Effects for Polymer Surface Discharges", in Reference 4, pp. 646-656.
7. Yadlowsky, E.J., Hazelton, R.C., and Churchill, R.J. "Characterization of Electrical Discharges on Teflon Dielectrics Used as Spacecraft Thermal Control Surfaces", in Reference 4, pp. 632-645.
8. Amore, L.J., and Eagles, A.E., "Materials and Techniques for Spacecraft Static Charge Control", in Reference 2, pp. 621-654.
9. Meulenberg, A., "Evidence for a New Discharge Mechanism for Dielectrics in a Plasma", in Reference 1, pp. 237-246.
10. Beers, B.L., Hwang, H.-C., Lin, D.L., and Pine, V.W., "Electron Transport Model of Dielectric Charging", in Reference 4, pp. 209-238.
11. Schultz, J.M. (Ed.), Properties of Solid Polymeric Materials, Parts A and B, Academic Press, New York 1977.
12. Budenstein, P.P., "Dielectric Breakdown in Solids", Report AD-A012 177, prepared for the U.S. Army Missile Command, Redstone Arsenal, Alabama, 20 December 1974.
13. Leadon, R., and Wilkenfeld, J., "Model for Breakdown Process in Dielectric Discharges", in Reference 4, pp. 704-710.
14. Jordan, E.C. and Balmain, K.G., Electromagnetic Waves and Radiating Systems, 2nd Edition, Prentice-Hall, New York, 1968, pp. 557-563.
15. Balmain, K.G., Cuchanski, M., and Kremer, P.C., "Surface Micro-Discharges on Spacecraft Dielectrics", in Reference 2, pp. 519-526.
16. Flanagan, T.M., Denson, R., Mallon, C.E., and Treadaway, M.J., "Effect of Laboratory Simulation Parameters on Spacecraft Dielectric Discharges", paper G-8 presented at the 1979 IEEE Nuclear and Space Radiation Effects Conference, Santa Cruz, California, July 17-20, 1979.
17. Inouye, G.T., and Sellen, J.M., "A Proposed Mechanism for the Initiation and Propagation of Dielectric Surface Discharges", in Reference 3, pp. 309-312.